

# Efficient continuous wave second harmonic generation pumped at 1.55 $\mu\text{m}$ in quasi-phase-matched AlGaAs waveguides

X. Yu, L. Scaccabarozzi and J. S. Harris, Jr.

*Solid State and Photonics Laboratory, Stanford University, Stanford, California 94305*  
[xjyu@snow.stanford.edu](mailto:xjyu@snow.stanford.edu)

P. S. Kuo and M. M. Fejer

*E. L. Ginzton Laboratory, Stanford University, Stanford, California 94305*

**Abstract:** We have fabricated quasi-phase-matched AlGaAs waveguides for continuous-wave second-harmonic generation (SHG) pumped around 1.55  $\mu\text{m}$ . We find that the losses, which limit the conversion efficiency of this type of waveguide, are resulted from two corrugations—the initial template corrugation and the regrowth-induced domain-boundary corrugations. We are able to reduce the waveguide loss by improving the growth conditions. The waveguide loss is 6-7 dB/cm at 1.55  $\mu\text{m}$ , measured using the Fabry-Perot method. A record internal SHG conversion efficiency of 23 %W<sup>-1</sup> for AlGaAs waveguides is achieved using a 5-mm-long waveguide with a pump wavelength of 1.568  $\mu\text{m}$ .

@2005 Optical Society of America

**OCIS codes:** (190.2620) Frequency conversion; (190.4360) Nonlinear optics, devices; (190.5970) Semiconductor nonlinear optics including MQW

---

## References and links

1. M. M. Fejer, G. A. Magel, D. H. Jundt, and R. L. Byer, "Quasi-phase-matched second harmonic generation: tuning and tolerances," *IEEE J. Quantum. Electron.* **QE-28**, 2631-2654 (1992).
2. L. A. Eyres, P. J. Tourreau, T. J. Pinguet, C. B. Ebert, J. S. Harris, M. M. Fejer, L. Becouarn, B. Gerard, and E. Lallier, "All-epitaxial fabrication of thick, orientation-patterned GaAs films for nonlinear optical frequency conversion," *Appl. Phys. Lett.* **79**, 904-906 (2001).
3. A. Fiore, V. Berger, E. Rosencher, P. Bravetti, and J. Nagle, "Phasematching using an isotropic nonlinear optical material," *Nature* **391**, 463-466 (1998).
4. A. Fiore, S. Janz, L. Delobel, P. van der Meer, P. Bravetti, V. Berger, E. Rosencher, and J. Nagle, "Second-harmonic generation at  $\lambda = 1.6 \mu\text{m}$  in AlGaAs/Al<sub>2</sub>O<sub>3</sub> waveguides using birefringence phase matching," *Appl. Phys. Lett.* **72**, 2942-2944 (1998).
5. S. Venugopal Rao, K. Moutzouris and M. Ebrahimzadeh, "Nonlinear frequency conversion in semiconductor optical waveguides using birefringent, modal and quasi-phase-matching techniques," *J. Opt. A: Pure Appl. Opt.* **6**, 569-584 (2004).
6. K. Moutzouris, S. Venugopal Rao, M. Ebrahimzadeh, A. De Rossi, V. Berger, M. Calligaro, and V. Ortiz, "Efficient second-harmonic generation in birefringently phase-matched GaAs/Al<sub>2</sub>O<sub>3</sub> waveguides," *Opt. Lett.* **26**, 1785-1787 (2001).
7. S. Venugopal Rao, K. Moutzouris, M. Ebrahimzadeh, A. De Rossi, G. Gintz, M. Calligaro, V. Ortiz, and V. Berger, "Measurements of optical loss in GaAs/Al<sub>2</sub>O<sub>3</sub> nonlinear waveguides in the infrared using femtosecond scattering technique," *Opt. Commun.* **213**, 223-228 (2002).
8. K. Moutzouris, S. Venugopal Rao, M. Ebrahimzadeh, A. De Rossi, M. Calligaro, V. Ortiz, and V. Berger, "Second-harmonic generation through optimized modal phase matching in semiconductor waveguides," *Appl. Phys. Lett.* **83**, 620-622 (2003).
9. S. Ducci, L. Lanco, V. Berger, A. De Rossi, V. Ortiz, and M. Calligaro, "Continuous-wave second-harmonic generation in modal phase matched semiconductor waveguides," *Appl. Phys. Lett.* **84**, 2974-2976 (2004).
10. S. J. B. Yoo, R. Bhat, C. Caneau, and M. A. Koza, "Quasi-phase-matched second-harmonic generation in AlGaAs waveguides with periodic domain inversion achieved by wafer-bonding," *Appl. Phys. Lett.* **66**, 3410-3412 (1995).
11. S. J. B. Yoo, C. Caneau, R. Bhat, M. A. Koza, A. Rajhel, and N. Antoniadis, "Wavelength conversion by difference frequency generation in AlGaAs waveguides with periodic domain inversion achieved by wafer

- bonding," *Appl. Phys. Lett.* **68**, 2609-2611 (1996).
12. C. Q. Xu, K. Takemasa, K. Nakamura, K. Shinozaki, H. Okayama, and T. Kamijoh, "Device length dependence of optical second-harmonic generation in AlGaAs quasiphase matched waveguides," *Appl. Phys. Lett.* **70**, 1554-1556 (1997).
  13. S. Koh, T. Kondo, Y. Shiraka and R. Ito, "GaAs/Ge/GaAs sublattice reversal epitaxy and its application to nonlinear optical devices," *J. Cryst. Growth.* **227/228**, 183-192 (2001).
  14. X. Yu, L. Scaccabarozzi, O. Levi, T. J. Pinguet, M. M. Fejer and J. S. Harris, "Template design and fabrication for low loss orientation-patterned nonlinear AlGaAs waveguides pumped at 1.55  $\mu\text{m}$ ," *J. Cryst. Growth.* **251**, 794-799 (2003).
  15. A much higher value is reported for pulsed operation but a pulse duty cycle factor has to be multiplied in order to convert a pulsed SHG efficiency to a CW SHG efficiency.
  16. H. Kroemer, "Sublattice allocation and antiphase domain suppression in polar-on-nonpolar nucleation," *J. Vac. Sci. Tech. B.* **5**, 1150-1154 (1987).
  17. R. S. Williams, M. J. Ashwin, T. S. Jones and J. H. Neave, "Ridge structure transformation by group-III species modification during the growth of Al,Ga.As on patterned substrates," *J. Appl. Phys.* **97**, 0449051-0449055 (2005).
  18. E. Gil-Lafon, J. Napierala, D. Castelluci, A. Pimpinelli, R. Cadoret, and B. Gérard, "Selective growth of GaAs by HVPE: keys for accurate control of the growth morphologies," *J. Cryst. Growth* **222**, 482-496 (2001).
  19. R. T. Feuchter and C. Thirstrup. "High precision planar waveguide propagation loss measurement technique using a Fabry-Perot cavity," *IEEE Photon. Technol. Lett.* **6**, 1244-1247 (1994).
- 

## 1. Introduction

GaAs is an attractive material for nonlinear optical wavelength conversion because of its high nonlinear coefficient, broad IR transparency range, and well developed epitaxial growth technologies. It is also desirable to fabricate GaAs/AlGaAs waveguides in order to take advantage of the high optical mode confinement to obtain high mixing efficiencies at moderate input powers. Because of the isotropic nature of GaAs, birefringent phase matching is not possible in conventional AlGaAs waveguides, thus various artificial approaches must be adopted. In contrast to bulk GaAs materials, in which phase matching has been achieved only by quasi phase matching (QPM) [1,2], a number of approaches have been investigated to achieve phase matching in waveguides, such as form-birefringence phase matching (BPM) [3-7], modal phase matching (MPM) [8, 9], and QPM [10-14].

Unfortunately, efficient nonlinear waveguide devices based on GaAs/AlGaAs system have not been realized regardless of the phase matching approaches because of the propagation loss at either the fundamental or second harmonic wavelength. In lossless waveguides, the generated output power and the normalized conversion efficiency (in  $\%W^{-1}$ ) are proportional to the square of the waveguide length for undepleted pumps. In lossy waveguides, the attenuation at both fundamental and second-harmonic wavelengths results in most of the second harmonic (SH) power inside the waveguides being generated near the input end of the waveguide but most of the SH power exiting the waveguide being generated close to the output end. The maximum conversion efficiency is obtained with an optimized waveguide length that depends on the loss at both wavelengths so that short devices (1~3 mm) were typically required in order to achieve highest (although still moderate) conversion efficiency. The lowest loss at 1.6- $\mu\text{m}$  wavelength, ~5 dB/cm, has been reported in an AlGaAs nonlinear waveguide phasematched using the BPM technique [5-8]. However, the loss at the SH wavelength in this structure is as high as 100 dB/cm, estimated from the low conversion efficiency observed in this type of waveguide. This loss probably comes from the absorption by levels introduced in the gap of AlGaAs during the oxidation of surrounding AlAs layers as well as the scattering due to the rough AlO<sub>x</sub>/AlGaAs interface [8]. It is not straightforward to devise a method to protect AlGaAs during oxidation and to improve the interface quality. The highest continuous wave (CW) equivalent SHG efficiency of BPM waveguide is around 7%/W [15].

Compared with other approaches, QPM waveguides based on orientation-patterned GaAs (OP-GaAs) are promising, since the adjacent domains differ in crystal orientation but have equal refractive indexes, and so no light scattering would occur at the domain boundaries if waveguide corrugation associated with orientation reversal can be reduced to negligible

levels. Unfortunately, in GaAs QPM waveguides, high loss, proportional to the square of the corrugation height, results from scattering from the corrugated waveguide core. High waveguide losses, varying from 30~100 dB/cm at ~770 nm, have been observed, due to large waveguide-core corrugation, by different research groups [11, 12, 14]. Most of the reported SHG conversion efficiencies for doubling 1.55- $\mu\text{m}$ -wavelength radiation in those waveguides grown by molecular beam epitaxy (MBE) are around  $10^{-4}$ ~ $10^{-3}$   $\text{W}^{-1}$  because of this loss [12-14].

With a lower template corrugation, Yoo et al obtained so far the highest internal CW SHG conversion efficiency ( $15\% \text{W}^{-1}$ ) using a 3-mm-long waveguide based on a wafer-bonded template and organometallic chemical vapor deposition (OMCVD) rather than MBE regrowth [11]. The propagation loss at 1.55  $\mu\text{m}$  is around 5.5 dB/cm, but the loss at SH wavelength is still as high as 25-45 dB/cm, which limits the conversion efficiency [10, 11]. Nonetheless, these results indicate that AlGaAs QPM waveguides with high conversion efficiency are possible if the waveguide loss can be reduced.

In this study, we fabricated orientation-patterned GaAs templates with low template corrugation, ~30-45 nm, and grew waveguides on these templates by MBE. We found that the waveguide corrugation comes partially from the original template corrugation, but more importantly, from the interface grooves evolving during the regrowth. We were able to reduce the waveguide corrugation by reducing the corrugation of the original template, and by optimizing the regrowth conditions.

## 2. Waveguides fabrication process

Figure 1(a) illustrates our QPM waveguide structure grown on an OP-GaAs template, as well as the mode profile at the fundamental wavelength, showing the contribution of initial template corrugation to the final waveguide corrugation. Figure 1(b) shows a cross-section parallel to the waveguide sidewalls so that the QPM domains are perpendicular to the cross-section plane. The whole structure is grown by MBE. During the template growth process, a layer of GaAs with a  $90^\circ$  rotation about the wafer normal [1] with respect to the GaAs substrate is deposited on the substrate via a thin intermediate Ge layer [2, 14]. After growth, the wafer is lithographically patterned and a chemical etching is performed to expose the alternate regions with different orientations to define the QPM period. The template corrugation forms after the chemical etching because of the height difference between the regions of opposite orientations. This corrugation is not smoothed during the waveguide growth and significantly contributes to the corrugation of the final waveguides if the initial corrugation is large. As indicated in Fig. 1, the template corrugation height is mostly determined by the thickness of GaAs grown on Ge. Due to the characteristic of polar-on-nonpolar growth, GaAs with two different orientations will possibly grow on Ge surface, resulting in the antiphase domains (APD) [16]. Single-phase GaAs is achieved by the self-annihilation of APDs under certain growth conditions. A large substrate-offcut angle is required to allow the occurrence of APD annihilation and a GaAs layer with a thickness higher than the size of APDs is also required in order to bury the APDs before the completion of GaAs growth on Ge. The typical GaAs thickness is larger than 100 nm, which makes the template corrugation not negligible in previous work. Thus, our first efforts were to reduce the template corrugation.

In our growth process, GaAs (001) wafers with  $1^\circ$  offcut towards (111)B are used, rather than the typically higher angle offcut wafers, e.g.  $4^\circ$ , because high-angle offcut wafers result in rough surfaces before Ge growth and large-size-APD defects that cannot be buried even after 100-nm GaAs deposited on Ge. On the other hand, by using the substrate with lower-offcut angle, the surface roughness is dramatically reduced. Unfortunately, the low-offcut angle also increases the complexity of single-phase GaAs growth on Ge. We managed to minimize the GaAs thickness (around 200-300Å) on Ge required to get single-phase GaAs by optimizing the growth conditions, including high temperature annealing of the Ge surface and using low  $\text{As}_2/\text{Ga}$  over-pressure ratio. The detailed growth procedure will be discussed in

other reports. The structure was taken out of the MBE chamber and chemical etching was performed to reveal the surface of the different GaAs phases after photolithography. The remaining template corrugation height ranges from 30 to 45nm, which is considerably smaller than our prior results [14] and those reported by other groups [13]. After chemical etching, the wafer was cleaned by alternate dipping into hydrochloric acid and hydrogen peroxide several times; then it was reloaded into the MBE machine and the regrowth is performed to deposit the waveguide core and cladding layers as shown in Fig. 1(b).

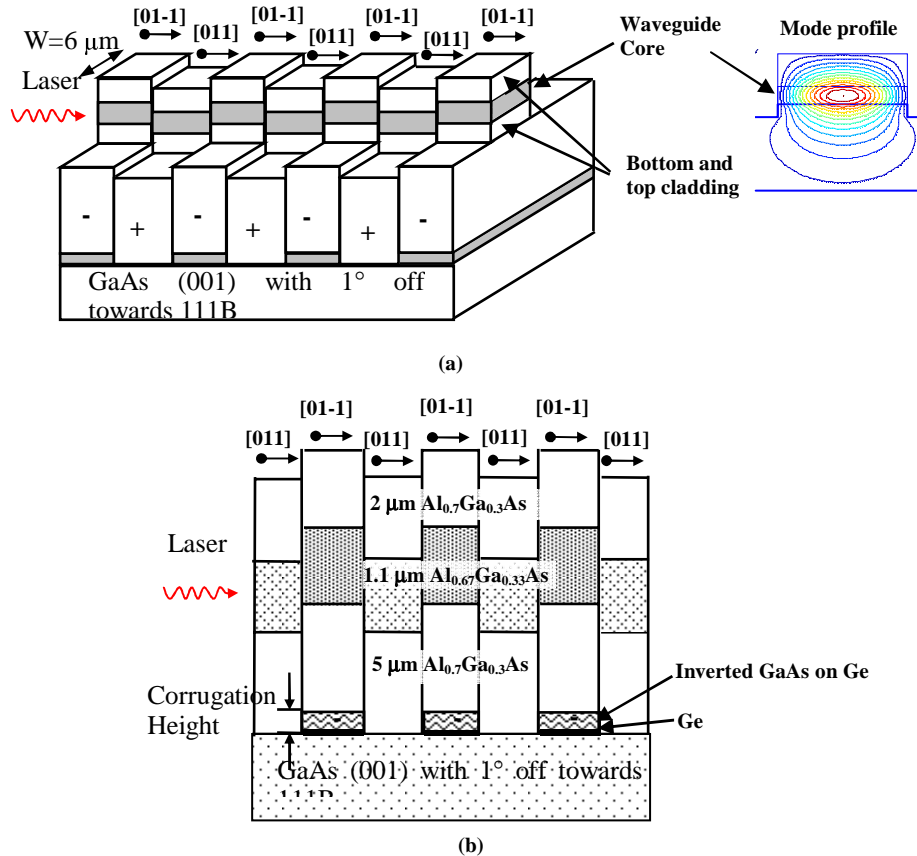


Fig. 1. QPM waveguide structures grown on an-orientation patterned GaAs template. Corrugations are undesired artifacts of the growth process.

The waveguide growth conditions were studied in order to improve the quality of the domain boundaries. We found that additional waveguide corrugation was induced because of the formation of interface grooves during waveguide growth. These grooves comprise the most significant part of the waveguide corrugation. Figure 2 shows scanning electron microscope (SEM) images of the cross section of the waveguides grown under two typical conditions. These two growth conditions differ only by the substrate temperature and have equal growth rate and V/III flux ratios. After growth, the sample is cleaved to obtain a cross section described in Fig. 1(b) so that the domain boundaries can be observed. The SEM image is taken without additional stain etching to reveal the domain boundaries. As shown in Fig. 2, the domain boundary is visible in as-cleaved samples and all the domains propagate vertically throughout the growth under both growth conditions. Deep v-shape grooves form on the domain boundary for the sample grown at 725°C. The depth of the groove is estimated to be 200-300 nm on the surface and a similar corrugation in the waveguide core is estimated. This magnitude is much larger than the original template corrugation and is expected to cause

the major part of the light scattering, and thus the propagation loss. This regrowth-induced corrugation was also observed in previous reports [10, 14], and possibly accounts for the unexpected high loss though the original template corrugation is low.

The formation of grooves on the phase boundaries can possibly be explained by the diffusion behavior of the adatoms. It is well known that the {111} surface of the GaAs has the lowest energy and that higher growth temperatures enable the diffusion of adatoms to form facets close to the equilibrium state that has been observed in GaAs growth on patterned structures [17, 18]. The formation of {111} faces on adjacent domains produces grooves on the interface. It is necessary to suppress the diffusion of surface adatoms to prevent the formation of grooves by using a lower growth temperature or higher V/III flux ratios. With a lower growth temperature, the v-shape grooves become almost invisible, as shown in Fig. 2. The remaining waveguide corrugation is then close to the original template corrugation, around 45nm. This corrugation height is very small compared with the waveguide core dimension and a low waveguide loss would be expected.

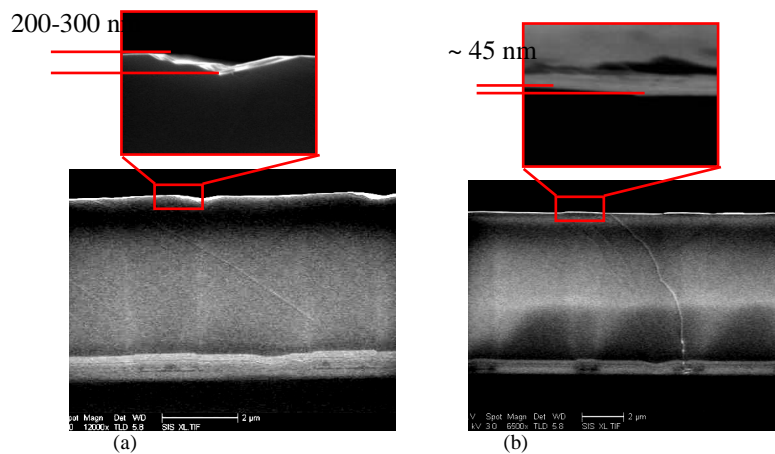


Fig. 2. Cross-section SEM of as-cleaved QPM waveguides under two different growth temperatures. Domain boundaries close to the surfaces are highlighted. (a) 725°C; (b) 665°C. Higher growth temperature results in large v-shape grooves at the domain boundaries while the low-temperature growth shows negligible waveguide corrugation.

After the MBE growth of the core and cladding structure, the waveguide pattern is defined by optical photolithography. Then, ridges are dry-etched in a  $\text{Cl}_2:\text{BCl}_3:\text{Ar}$  plasma using a Plasmaquest Electron Cyclotron Resonance (ECR) enhanced Reactive Ion Etcher (RIE), as shown in Fig. 1(a). This dry etching technique produces extremely vertical and smooth sidewalls. The top cladding and the core are etched through, resulting in a ridge height of  $\sim 3.5 \mu\text{m}$ . A single-mode profile at the fundamental wave as shown in Fig. 1(a) is obtained for the waveguides narrower than  $8 \mu\text{m}$  and the  $1/e^2$ -intensity-width of this mode is  $\sim 4.4 \mu\text{m}$  for a  $5.8\text{-}\mu\text{m}$ -wide waveguide. In the end, after removing the photoresist used as dry etching mask, the waveguides were cleaved in various lengths for loss and SHG testing.

### 3. Results

The loss at the fundamental wavelength of  $1.55 \mu\text{m}$  with TE-mode input was measured using the Fabry-Perot method [19]. The loss of the sample grown at  $725^\circ\text{C}$  is  $\sim 15\text{-}20 \text{ dB/cm}$  for the patterned waveguides and  $\sim 2\text{-}3 \text{ dB/cm}$  for the unpatterned waveguide on the same wafer. The variation of loss with different waveguide width from  $6 \mu\text{m}$  to  $14 \mu\text{m}$  for the patterned waveguides is below  $2 \text{ dB/cm}$ . This width independence of the loss suggests that the sidewall roughness contributes only a small fraction of the waveguide loss and that the dominant factor

is waveguide corrugation. On the other hand, the loss of the sample grown at 665°C is ~6-7 dB/cm for the patterned waveguides and ~3-4 dB/cm for the unpatterned ones. The difference between the patterned waveguide and unpatterned waveguides can be explained by remaining template corrugation; this corrugation is no longer the dominant factor that induces loss in these waveguides. Since the low temperature and high temperature grown waveguides were grown on OP-GaAs templates with equal template corrugation height, we can conclude that the high waveguide loss is determined by the waveguide corrugation formed during the regrowth rather than by original template corrugation. In this case, we can expect even better QPM waveguides if we can further suppress the template corrugation by optimizing the growth condition of the OP-GaAs template.

The waveguides grown at 665°C were tested by employing a fiber-coupled tunable external-cavity-diode laser (tunable around 1.55  $\mu\text{m}$ ) amplified by an EDFA as the pump source. A polarizer and an in-line polarization controller control the polarization before the light is coupled into the waveguides. With a beam sampler monitoring the input power, the beam is coupled in and out of the waveguides using high numerical aperture (NA=0.65) aspheric lenses. Type I SHG is tested with the fundamental input TE-polarized and SH output TM-polarized. We record SH power after the output coupling lens as a function of the wavelength using a lock-in amplifier to increase the signal-to-noise ratio.

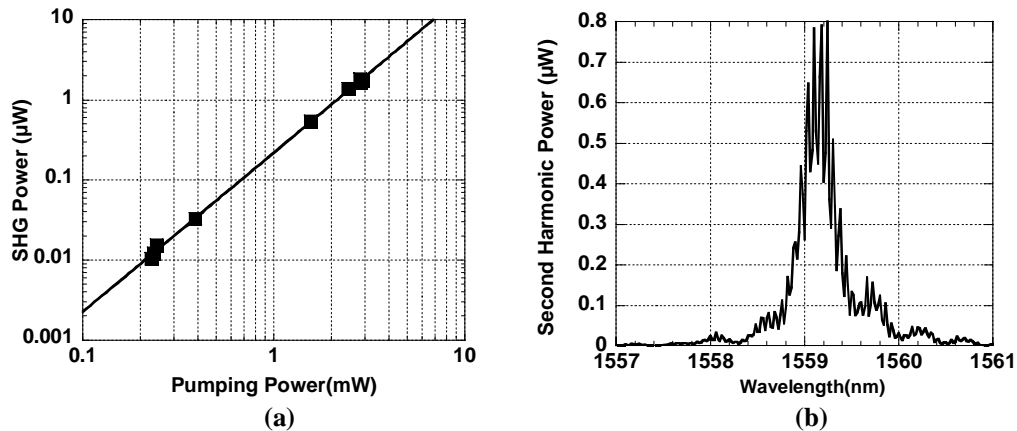


Fig. 3. (a) Relationship between SHG output power and fundamental input power. (b) SHG output power vs tuning of the fundamental wavelength. The input power is measured at 4.25mW in front of the input facet. Fringes are due to Fabry-Perot resonances at the pump wavelength.

The highest conversion efficiency is achieved using a 5-mm-long and 5.8- $\mu\text{m}$ -wide waveguide. The optimum length is longer than prior reports due to the reduced waveguide loss. Figure 3(a) shows the SH output power vs the fundamental input power on a logarithmic scale; the slope is close to 2. This result indicates that the SH power has a quadratic dependence on the input power as expected for undepleted pump SHG. Figure 3(b) shows a typical second-harmonic tuning curve recorded with 4.25-mW input fundamental power (the power in front of the waveguide input facet), for a waveguide with a core of 1.1- $\mu\text{m}$   $\text{Al}_{0.63}\text{Ga}_{0.37}\text{As}$  and cladding of  $\text{Al}_{0.66}\text{Ga}_{0.34}\text{As}$ , and a QPM period equal to 4.7  $\mu\text{m}$ . The SH generation peaks at 1559.1 nm with the peak-power value at ~0.61  $\mu\text{W}$  after removing the Fabry-Perot enhancement effect. The full width at half-maximum (FWHM) is ~0.37 nm, which is narrower than prior results due to the increased interacting lengths, but is about twice of the simulated ideal value (~0.19 nm) in a lossless waveguide because of the waveguide losses.

The external SHG conversion efficiency is ~3.4 %  $\text{W}^{-1}$  based on Fig. 3. Internal conversion efficiency is calculated to compare with previous reports. Several factors are taken into account. The input power is recorded as the power in front of the input facet; the actual power

coupled into the waveguide is only a fraction of the measured power because of the Fresnel reflection at the input facet and because of the overlap efficiency between the free space Gaussian mode and the waveguide mode. The input coupling coefficient is ~45%, which is obtained based on the measurement of the transmission of short (~1 mm) low-loss plain waveguides with same widths and is also close to the theoretical calculation. The recorded SH power is about 72% of the actual SHG power generated in the waveguide because of end-facet reflection at the SH wavelength. Counting all the factors above, we obtained 0.85- $\mu$ W internal-SH output with 1.91-mW internal-fundamental input. This output corresponds to a normalized internal conversion efficiency of 23 %W<sup>-1</sup>, which is the highest ever reported for doubling 1.55  $\mu$ m under CW operation in AlGaAs waveguides. The ideal internal SHG efficiency is 125%W<sup>-1</sup> for a 5-mm-long lossless QPM waveguide with the same structure as the waveguide characterized here. The reduction of the conversion efficiency can be accounted for by the waveguide loss and the QPM duty-cycle error. The loss at 1.56  $\mu$ m is measured to be 6.7 dB/cm. By fitting of the theoretical tuning curve with the experimental tuning curve, we obtained an estimated loss at 780 nm to be 13-15 dB/cm. With this loss, the theoretical internal conversion efficiency is reduced to 27 %W<sup>-1</sup>, which is close to our measured value.

#### 4. Conclusions

In conclusion, we fabricated low-loss orientation-patterned QPM AlGaAs waveguides using MBE. The waveguide corrugations were identified as the dominant loss mechanism, which contain two parts: one part comes from the original template corrugation and the other part forms during the regrowth, where the effect of the latter one was not well recognized in prior works. We reduced the waveguide loss by minimizing both corrugations. The loss at 1.55  $\mu$ m is ~6-7dB/cm, which is close to the loss of unpatterned waveguides fabricated by the same process. The loss at 780 nm is ~13-15 dB/cm, which is the lowest value that has been achieved for OP-GaAs QPM waveguides. Record-high internal conversion efficiency of 23 %W<sup>-1</sup> in AlGaAs nonlinear waveguides has been achieved with a 5-mm-long waveguide. Although AlGaAs QPM waveguides are still less efficient than current LiNbO<sub>3</sub> nonlinear waveguides, the conclusions on corrugation-reduction obtained in this report allow us to further improve the waveguide quality and reduce the losses at both fundamental and SH wavelengths. Thus, continuous improvement of the conversion efficiency is expected, which can possibly lead to the practical applications of AlGaAs nonlinear waveguides in the future, especially in the wavelength range where LiNbO<sub>3</sub> is not transparent.

#### Acknowledgments

This work was supported by the U. S. Air Force Office of Scientific Research under grant F49620-01-1-0428. X. Yu acknowledges the support from the Winston and Fu-Mei Chen Stanford Graduate Fellowship.